sciendo

Archives of Hydro-Engineering and Environmental Mechanics
Vol. 67 (2020), No. 1–4, pp. 17–34
DOI: 10.1515/heem-2020-0002
ISSN 1231–3726

Experimental Investigation of Skirted Foundation in Sand Subjected to Rapid Uplift

Marek Kulczykowski

Institute of Hydro-Engineering, Polish Academy of Sciences, 7 Kościerska, 80-328 Gdańsk, Poland,
e-mail: marek@ibwpan.gda.pl

(Received November 03, 2020; revised December 02, 2020)

Abstract

This paper reports results from 1g model tests carried out under single gravity on a skirted foundation installed in sand and subjected to a rapid uplifting force. The effects of displacement rates ranging from 5 mm/s to 450 mm/s on the ultimate capacity, suction pressure inside the skirt compartment, and time of extraction were investigated. Test results indicate that the displacement rate significantly affected the magnitude of uplift resistance, as well as the magnitude of suction under the foundation lid, but had little effect on the relationship between stress and the displacement of the foundation. The shapes of the uplift capacity-displacement curve and the suction-displacement curve were similar for all experimental displacement rates.

Key words: skirted foundation, suction caisson, pullout resistance, rapid uplift, model investigations

Notation

a – parameter of power function,
A – cross-sectional plane area of the skirt foundation model,
D – inner diameter of the foundation,
D_{10} – effective size of soil particles,
D_{60} – 60% of soil particles are smaller than this size,
E – void ratio,
$e_{\min}$ – minimum void ratio,
$e_{\max}$ – maximum void ratio,
G_c – weight of the skirted foundation,
G'_c – buoyant weight of the skirted foundation,
G_s – specific gravity of sand particles,

h – skirt inner length,
k_0 – coefficient of permeability,
q – uplift capacity,
q_{net} – net uplift capacity,
Q – uplift force,
$Q_{\max}$ – peak uplift force,
t_c – time of complete pullout from the subsoil,
t_i – time of the initial stage of pullout,
t_f – time of the final stage of pullout,
t_{skirt} – skirt thickness,
v – displacement rate,
w – vertical displacement
x, y – variables of the power function,
γ – unit weight of dry sand,
γ_{sat} – unit weight of saturated sand,
γ' – buoyant unit weight of saturated sand,
δ – friction angle between the soil and the model wall,
ϕ – internal friction angle.

1. Introduction

Skirted foundations, also known as suction caissons, are steel or concrete cylinders that are closed at the top and open at the bottom. These types of foundations are used in a variety of offshore structures, such as oil and gas platforms or wind turbines (Randolph et al 2011, Tjelta 2015). The main benefit of using these modern technological solutions in geotechnical engineering is their capability of withstanding high foundation loads, which generally press the foundation down into the seabed, but may also pull it out of the subsoil. Skirted foundations are capable of withstanding rapid tensile loading due to suction generated between the top plate and the soil plug confined by the skirts (Fig. 1).

A number of studies have been performed to investigate the response of the skirted foundation in sand during its installation and under compressive or tensile loading. Byrne (2000) has reviewed field trials and presented a historical sequence of field testing of suction caissons. The state-of-the-art laboratory testing of skirted foundation under loading has been described by Manzzotti et al (2014). Various theoretical and experimental investigations have been carried out into foundations subjected to uplift loading. Theoretical solutions and procedures for estimating the pullout capacity of skirted foundations in sand are proposed by Houlsby et al (2005), Senders (2008), Lehane et al (2014) and Sawicki et al (2016). Numerical analyses have been performed by Rahman et al (2001), Zhou et al (2008), Mana et al (2014), Thieken et al (2014), and Shen et al (2017). A recent experimental study in a centrifuge is presented in (Wang et al 2019), and pullout capacities measured in 1g model tests are reported by

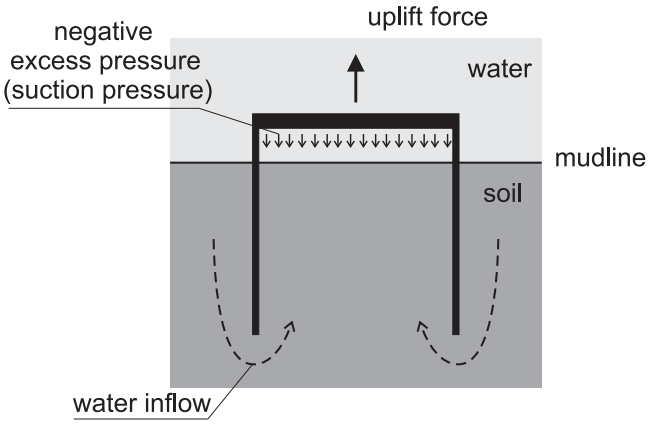

Fig. 1. Suction generation between the top plate of the skirted foundation and the soil plug confined by the skirts

Kelly et al (2004), Luke et al (2005), Kakasoltani et al (2011), Hung et al (2017), Zhai and Li (2017), and Xie et al (2020).

In recent years, there has been a worldwide pressure to develop new sources of renewable energy. One of viable sources of renewable power is wave energy converted into electricity by Wave Energy Converters (WECs) (Aderinto and Li 2019). These devices, activated by the cyclic oscillation of waves, are permanently or partially submerged in water (Fig. 2) and thus subjected to uplift. Skirted foundations are therefore a good solution for supporting WEC structures. On the other hand, such structures, which are fully immersed in water, are exposed to substantial tensile loads under stormy conditions.

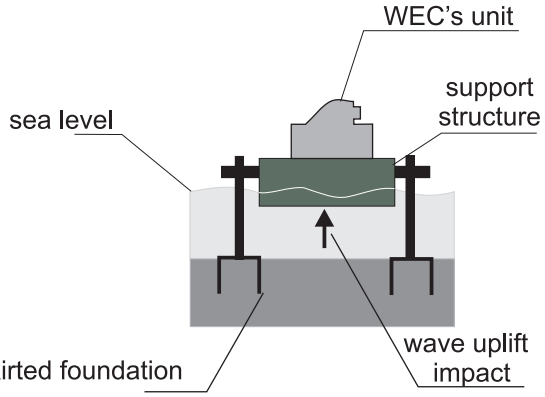

Fig. 2. Sketch of a WEC-supporting structure with skirted foundations

The Institute of Hydro-Engineering of the Polish Academy of Sciences in Gdańsk has monitored and carried out field measurements of the sea surface under stormy conditions at south Baltic locations. Wave data from wave buoys in the Polish coastal

zone (Ostrowski et al 2016) indicate that waves reached heights of 2.5–7 m under storm conditions, while the average vertical velocity of waves (the vertical component of water particle velocity on the sea surface) ranged from 620 to 1300 mm/s depending on storm intensity. It could be expected that the structure will be rapidly extracted from the subsoil when the relevant holding capacity of the foundation is exceeded under stormy conditions. However, laboratory pullout tests are usually performed at relatively low displacement rates, lower than 10 mm/s, and there is a lack of experimental investigations of the response of skirted foundations to rapid extraction from the seabed.

This paper reports results from 1g model tests of a skirted foundation in sand subjected to rapid tensile loading. The effects of high rates of displacement, ranging from 5 mm/s to 450 mm/s, on the ultimate capacity, suction pressure inside the skirt compartment, and time of extraction were investigated.

2. Test and Loading Arrangements

The tests with a skirt foundation model were carried out in a test container filled with sand and water. The circular steel model was installed in a fully saturated soil and then pulled out. The inside diameter of the foundation was $D = 100$ mm, the skirt inner length was $h = 100$ mm, and the wall thickness was $t_{skirt} = 1.5$ mm. Hence the embedment ratio (the skirt depth to foundation diameter ratio) was $h/D = 1$, and the skirt thickness to diameter ratio was $t_{skirt}/D = 0.015$. The cross-sectional area of the foundation was $A = 7.85 \times 10^{-3}$ m^2. The own weight of the model was $G_c = 8.4$ N, and its buoyant own weight was $G'_c = 7.2$ N. The model was equipped with an air release valve for dissipation of internal excess air pressure during installation and a water pressure sensor for measurement of suction beneath the lid during the experiment (Fig. 3).

The tests were performed in a circular tank (diameter = 600 mm, depth = 730 mm). A pneumatic pullout loading system was used. The foundation was connected to a vertical pullout loading arm with a load cell, which in turn was connected to a vertical actuator. The uplift displacement was measured by a vertical displacement transducer.

Before all tests, the tank was filled with water to a depth of 45 cm, and then sand was rained from the top with a sieve. Sand was rained from an average height of 5 cm above the water level to obtain a uniform density. This method also ensured the full saturation of soil and limited the possibility of water aeration. When the soil deposit was 400 mm in height, the tank was filled up with water to a level of 150 mm above the sand surface. A diagram of the test setup is presented in Figure 4.

The soil used in the tests was collected from a beach near the village Lubiatowo (latitude 54.796 N, longitude 17.867 E) on the Baltic sea. The density of dry and saturated sand was determined by measuring the weight and volume of the sample. The value of the angle of friction was obtained in a triaxial test. The interface friction

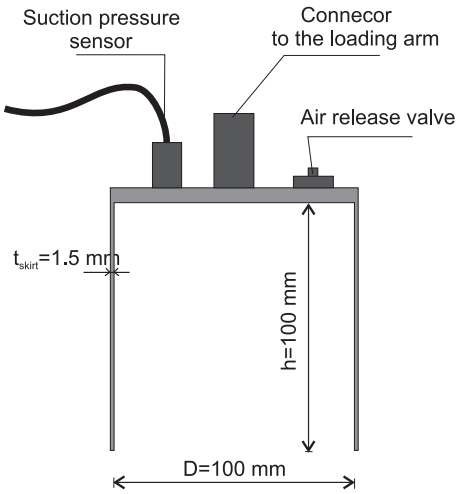

Fig. 3. Model geometry and equipment

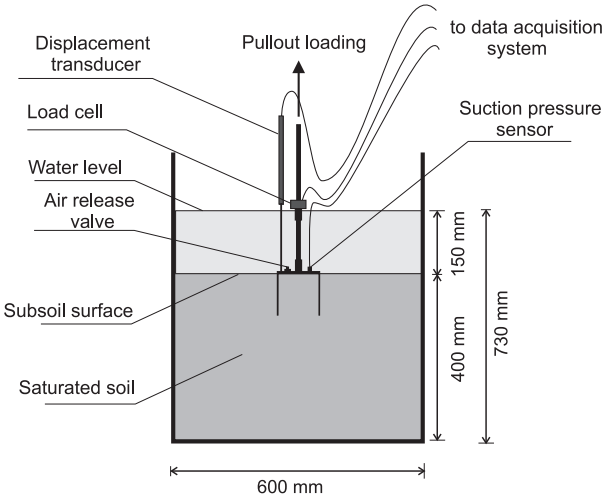

Fig. 4. Diagram of the test setup and measurement system

angle between the caisson wall and the soil was determined using a direct shear apparatus. Figure 5 shows the particle size distribution curve, and Table 1 summarizes the properties of the test sand. The soil sample was classified as non-cohesive fine silica sand.

3. Testing Program

Seven 1g tests were carried out to study the response of the skirted foundation to a rapid pullout process. The installation process was similar in all experiments. The foundation was installed concentrically in the saturated subsoil with the drainage valve

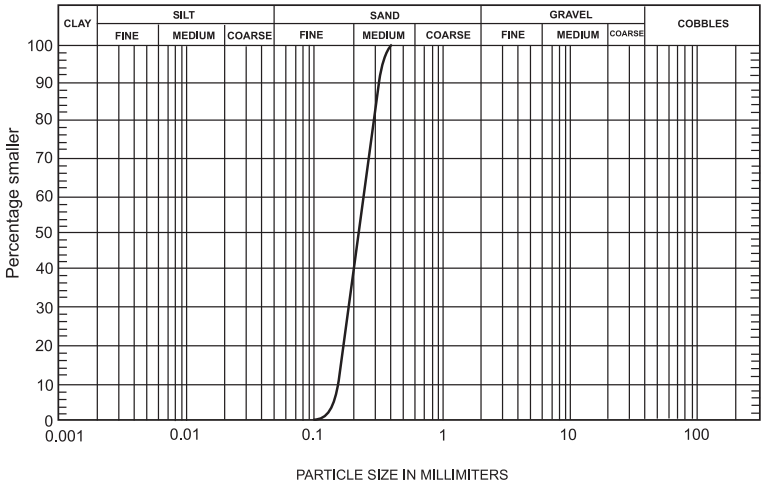

Fig. 5. Particle size distribution curve of Lubiatowo sand

Table 1. Properties of Lubiatowo sand

D_{10}	0.15 mm
D_{60}	0.25 mm
Specific gravity of sand grains G_s	2.58
Unit weight of dry sand γ	15.8 kN/m^3
Unit weight of saturated sand γ_{sat}	19.7 kN/m^3
Buoyant unit weight of saturated sand γ'	9.7 kN/m^3
Internal friction angle ϕ	34.0°
Friction angle between the soil and the model wall δ	9.7°
Void ratio e	0.64
Minimum void ratio $e_{\min}$	0.55
Maximum void ratio $e_{\max}$	0.82
Density index I_D	0.6
Coefficient of permeability k_0	1.54×10^{-3} m/s

kept open to release the air trapped inside the model. First, the model was pressed down by the actuator at a displacement rate of $v = 2$ mm/s (which was relatively low compared to the pullout process) to a depth of 70% of the skirt length. Next, in order not to overload the soil, the installation was continued manually until the foundation was completely embedded in the subsoil. Then the foundation was sealed by closing the drainage valve, and an axially-symmetric pullout force was applied. The pull-out force, the displacement of the foundation, and pressure inside the model were recorded. In all tests, the model was completely pulled out of the soil. The measurements were made until the foundation lid reached the water level. After experiments, the foundation was examined to determine whether a sand plug remained inside the skirt compartment.

4. Results

The results of the experiments are summarized in Tables 2 and 3 and presented in Figures 6 to 18. The uplift capacity is taken as the load cell reading Q divided by the plan area A of the foundation: $q = Q/A$. The uplift displacement of the foundation is presented in the normalized form w/D (in percentages) as the vertical displacement w divided by the foundation diameter D or in the form of the relative displacement w/h, where h is the skirt depth. As the skirt depth to diameter ratio is $h/D = 1$, normalized and relative displacements have the same values.

The subsequent tests were performed at seven different preset displacement rates of 5 mm/s, 8.5 mm/s, 19 mm/s, 30 mm/s, 110 mm/s, 250 mm/s, and 450 mm/s. It should be noted that these were so-called protective pullout rates, i.e. the fastest possible velocities that the piston rode of the actuator was allowed to reach in a given test. In all tests, however, the value of the displacement rate changed during the experiment. In the initial stage of the experiment, the displacement rate was close to zero and then increased during extraction to the preset value. The model was extracted at this displacement rate after the peak of the uplift capacity was reached. Figure 6 shows an example of changes in uplift displacement and uplift capacity over time in a test with a preset displacement ratio of 110 mm/s.

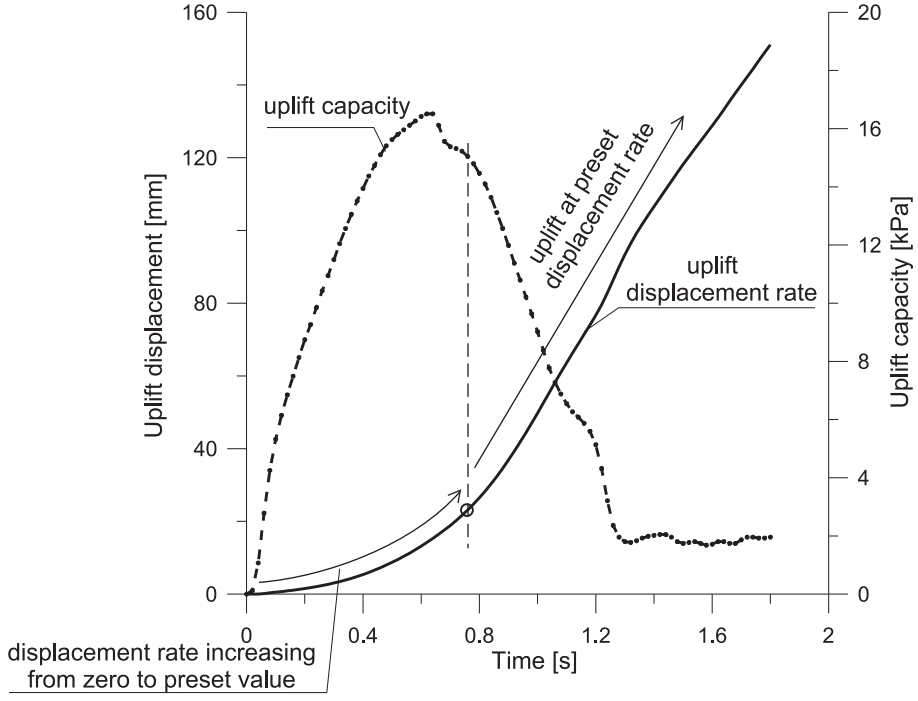

Fig. 6. Comparison of changes in uplift displacement and uplift capacity over time at a preset displacement ratio of 110 mm/s

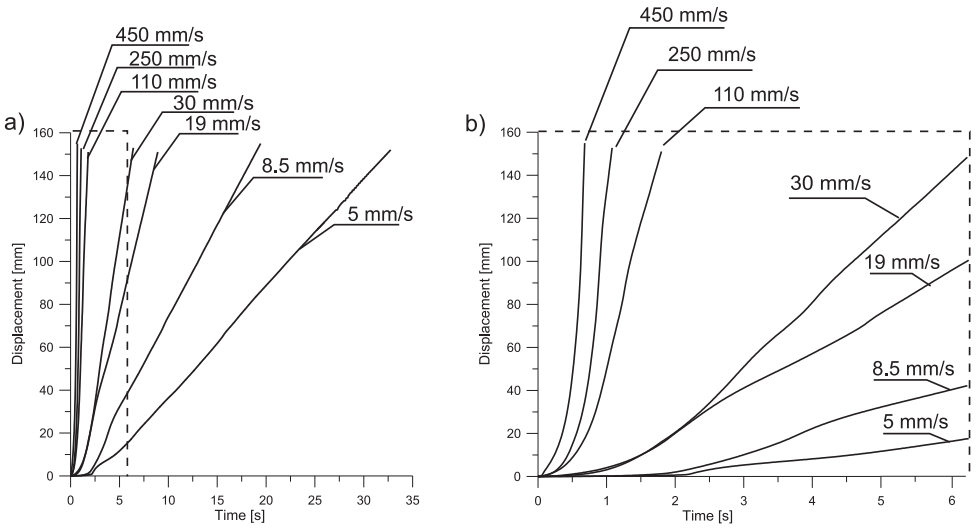

Fig. 7. Variation in uplift displacement rates during particular experiments

The displacement rates observed in all tests are shown in Figure 7a. For clarity, the part of this figure separated by dashed lines is presented in Figure 7b. During all tests, the displacement rate changed in a way similar to that described above in the experiment at a preset uplift rate of 110 mm/s.

The effects of displacement rates on uplift capacity and suction pressure in the skirt compartment are presented in Figures 8 to 10. In all experiments, similar changes were observed in uplift capacity and suction during the pullout process. The results of the experiment carried out at a preset displacement rate of 110 mm/s are presented in Figures 8a, b as an example. Figure 8a depicts a stress-displacement response of the foundation during uplift, and Figure 8b shows the corresponding values of negative pressure measured under the base plate.

The uplift capacity increased rapidly before the peak value was reached. At this first stage of pullout, the uplift displacement of the foundation was initially very small and then increased until the ultimate uplift capacity of the foundation was developed. At this phase of the pullout process, the displacement rate increased from zero to the preset value. Thereafter, at the final stage of extraction, the uplift capacity decreased gradually with continued pullout to a residual level, which was reached after complete extraction from the subsoil.

The pullout process resulted in creation of negative excess pressure (suction) beneath the foundation lid. Changes in uplift capacity and suction pressure during extraction were similar, but absolute values of suction were slightly smaller than the corresponding values of uplift resistance. At the initial stage of extraction, suction developed up to a maximal value, and at the final stage the loss of suction was observed. The maximum of uplift capacity and the maximum of suction beneath the lid occurred at the same time. It is marked by dashed lines in Figures 8a, b.

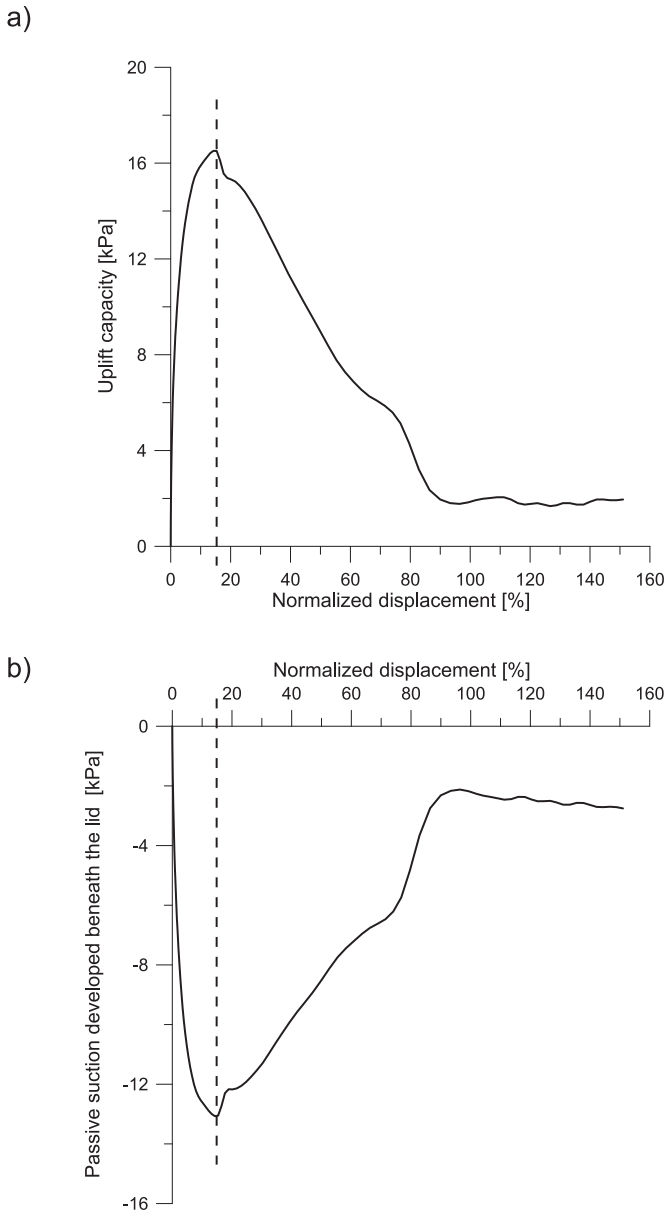

Fig. 8. Typical measurement of (a) uplift capacity and (b) excess of negative pressure (suction) beneath the lid versus normalized displacement (test performed at a pullout rate of 110 mm/s)

The stress-displacement responses of the foundation during uplift recorded in all tests are compared in Figure 9. The corresponding changes in suction plotted against normalized displacement are shown in Figure 10.

The ultimate capacity, maximum suction beneath the lid, and foundation displacement at the ultimate capacity increased significantly with increase in displacement

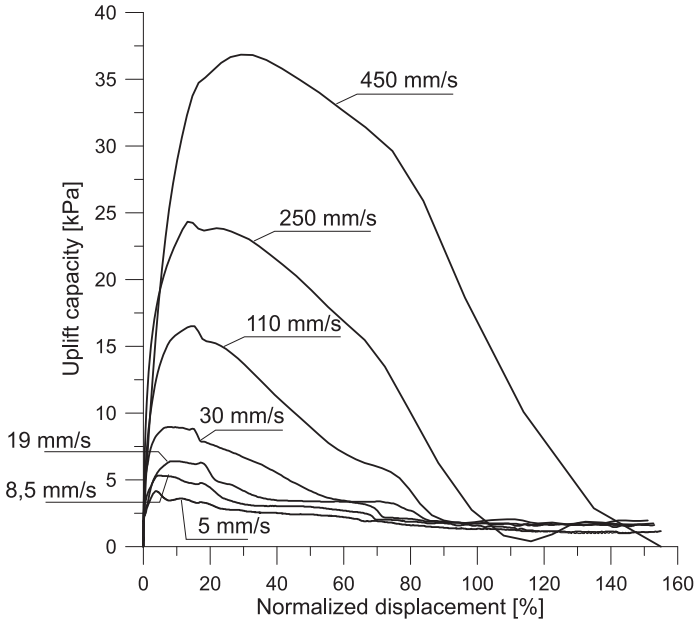

Fig. 9. Uplift capacity versus normalized displacement for experimental displacement rates

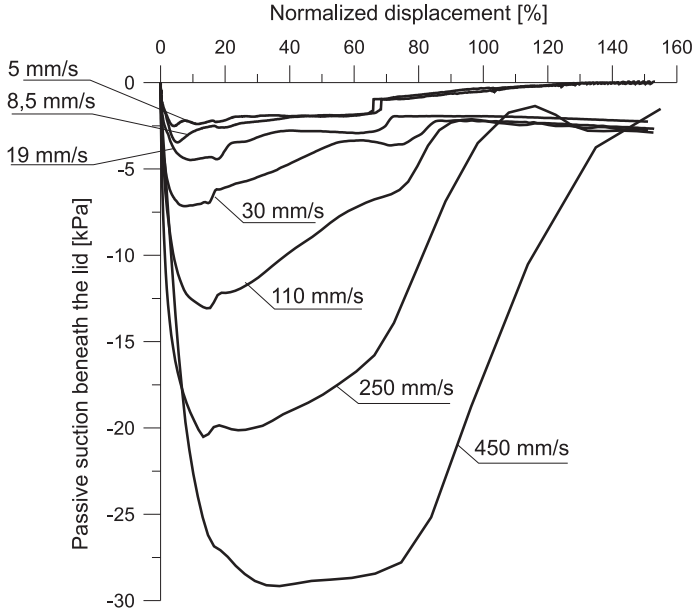

Fig. 10. Suction pressure versus normalized displacement for experimental displacement rates

rate. However, the uplift capacity-displacement curve and the suction-displacement curve exhibited similar shapes in all tests. Analogous changes in uplift resistance and suction during pullout were also observed in experiments with lower displacement rates (see Kakasoltani et al (2011) and Wang et al (2019)). Therefore, it can be concluded that the displacement rate has a small effect on the stress-displacement relationship of the skirted foundation, but significantly affects the magnitude of uplift capacity as well as the magnitude of suction in the skirt compartment.

The time histories of uplift capacity for all experimental displacement rates are presented in Figure 11a. In order to improve the readability of the graph, the results obtained for lower displacement rates (5 mm/s, 8.5 mm/s, 19 mm/s, and 30 mm/s) are presented in Fig. 11b, and the results recorded at higher experimental uplift rates are shown in Figure 11c. The cross mark on the curves in Figures 11b,c denotes the time period tc from the beginning of pullout to the moment when the foundation completely separated from the subsoil (at normalized displacement equal to 100%). Let us recall that the experimental measurements were stopped when the foundation lid reached the water level. At that time, the bottom rim of the skirt was 50 mm above the subsoil surface.

The period t_c and the durations of initial and final stages of extraction, denoted as t_i and t_f respectively, are summarized in Table 2 and illustrated in Figure 12. For the record, at the initial stage of pullout, uplift capacity increased to the peak value, whereas at the final stage, it decreased to the residual value. The value of t_f is the difference between t_c and t_i $\left(t_f = t_c - t_i\right)$.

Table 2. Summary of time measurements

Displacement rate v [mm/s]	Duration of complete pullout from the subsoil t_c [s]	Duration of the initial stage of pullout t_i [s]	Duration of the final stage of pullout $t_f = t_c - t_i$ [s]
5	22.2	2.58	19.6
8.5	13.1	2.32	10.8
19	6.3	1.42	4.9
30	4.6	1.30	3.3
110	1.4	0.62	0.8
250	0.9	0.50	0.4
450	0.6	0.42	0.2

The displacement rate significantly affected the values t_c, t_i, and t_f, which decreased with increasing preset displacement rate. At lower displacement rates, however, the duration of the initial stage of pullout ti was considerably greater than the duration of the final stage t_f. These differences between t_i and t_f decreased for higher uplift rates (see Fig. 13).

As already mentioned, the model was examined after the experiment to check whether the sand plug was removed from the subsoil within the foundation. At the two

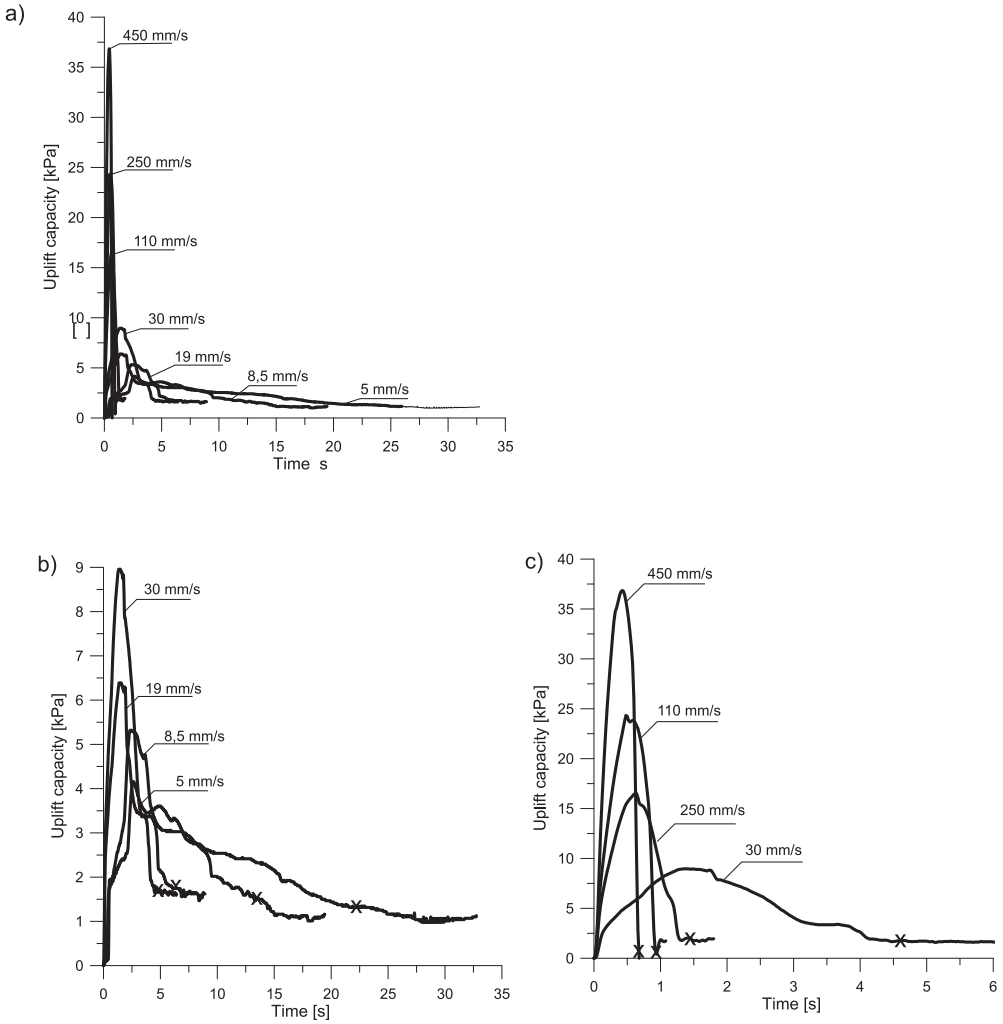

Fig. 11. Time histories of uplift capacity during pullout: (a) for all experimental displacement rates; (b) for rates of: 5 mm/s, 8.5 mm/s, 19 mm/s, and 30 mm/s; (c) for rates of: 30 mm/s, 110 mm/s, 250 mm/s, and 450 mm/s

lowest displacement rates (5 mm/s and 8.5 mm/s), no sand plug was observed inside the foundation after extraction. At all higher uplift rates, the sand plug was pulled out in the skirt compartment, which resulted in greater residual uplift capacities in the final stage of lifting (Fig. 14).

The extracted soil was released from the foundation after the air release valve was opened. This indicated the presence of a residual negative pressure beneath the lid. In all tests, the weight of retained soil was about 9 N, and about 80% of the skirt compartment was filled with captured sand.

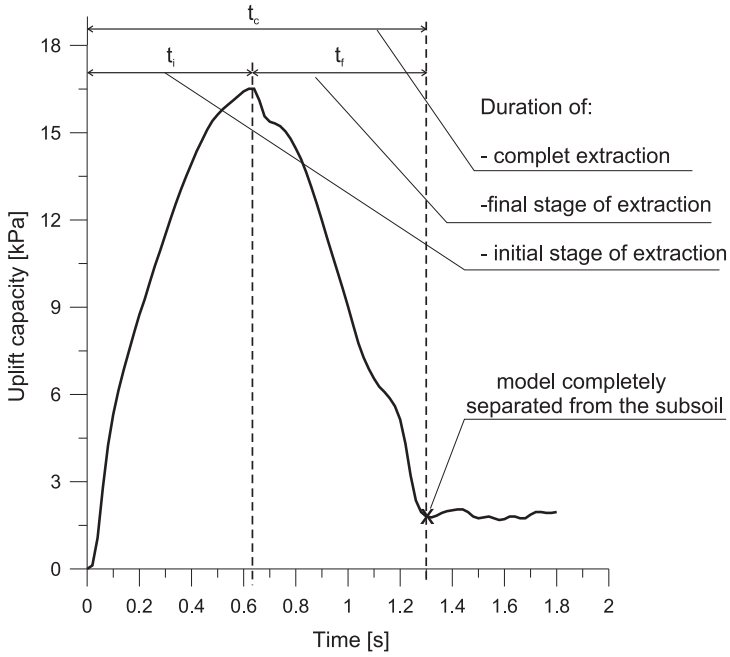

Fig. 12. Periods t_c, t_i, and t_f in a typical measurement of uplift capacity during extraction (at a displacement rate of 110 mm/s)

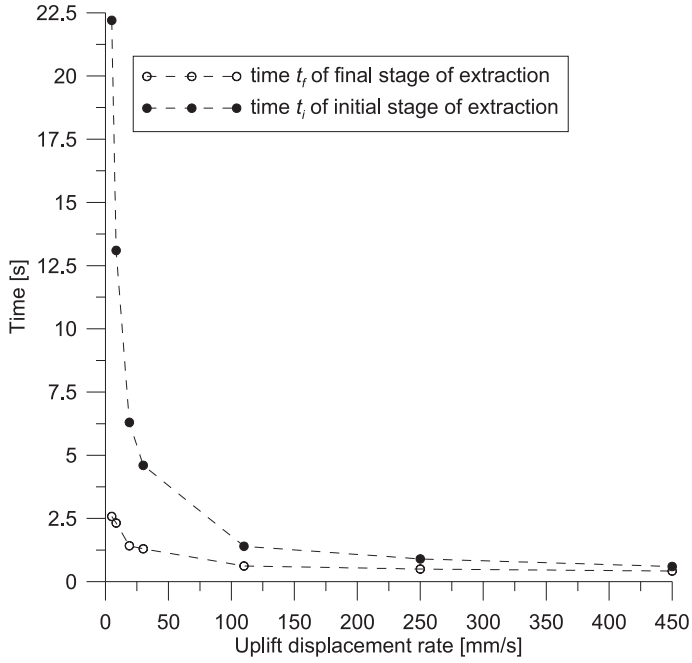

Fig. 13. Times t_f and t_i vs. displacement rate

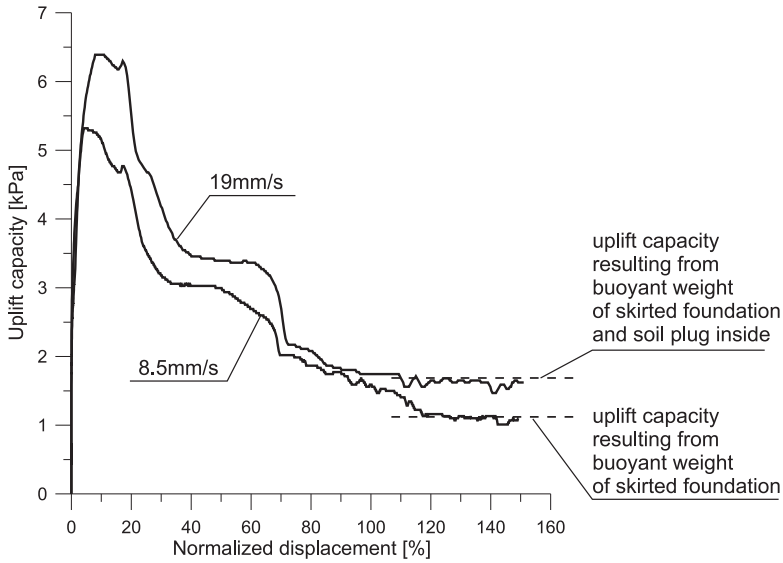

Fig. 14. Measurements of uplift capacity from tests with and without a sand plug inside the model after extraction

A summary of pullout data recorded for all preset displacement rates is presented in Table 3. The ultimate capacity q_u is taken as the maximal uplift force $Q^{\max}$ divided by the plan area A: $q_u = Q^{\max}/A$. The net ultimate capacity q_{net-u} corresponds to the difference between $Q^{\max}$ and the buoyant own weight of foundation G'_c presented in terms of stresses: $q_{net} = (Q - G'_P)/A$. The values of ultimate suction pressure and normalized displacement correspond to the peak uplift capacity.

The ultimate capacity and the corresponding peak values of suction pressure varying with the displacement rate are presented in Figures 15 and 16, respectively. Variation in normalized displacement recorded at the peak uplift capacity with the displacement rate is shown in Figure 17.

The values of the ultimate capacity and uplift displacement, as well as the absolute values of peak suction pressure, increased significantly with increasing preset

Table 3. Summary of pullout data recorded for all preset displacement rates

Displacement rate [mm/s]	Ultimate capacity q_u [kPa]	Net ultimate capacity q_{net-u} [kPa]	Suction pressure at ultimate capacity [kPa]	Normalized displacement at ultimate capacity [%]	Sand plug extracted
5	4.16	3.24	−2.49	3.6	no
8.5	5.32	4.40	−3.68	4.23	no
19	6.39	5.47	−4.47	7.9	yes
30	8.96	8.04	−7.16	8.2	yes
110	16.51	15.59	−13.07	13.2	yes
250	24.34	23.42	−20.13	16.4	yes
450	36.84	35.92	−29.16	26.1	yes

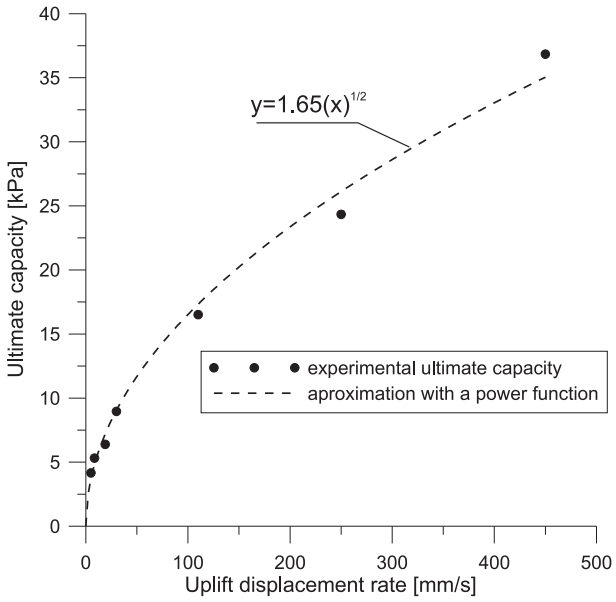

Fig. 15. Ultimate capacity varying with uplift displacement rate

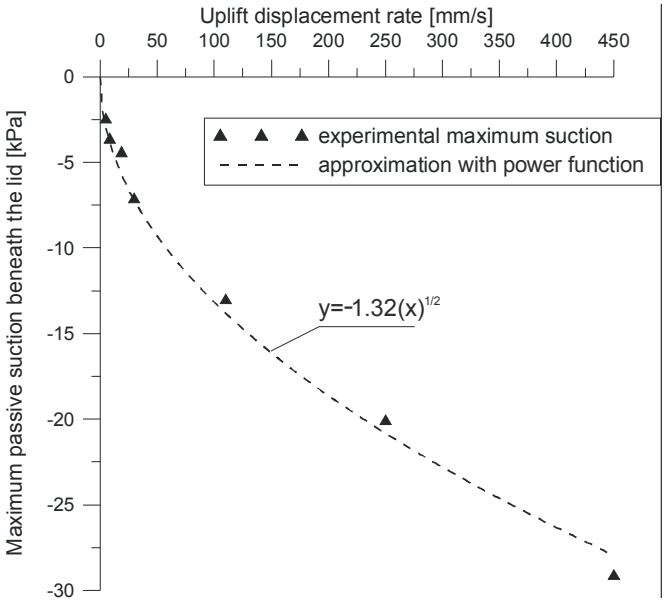

Fig. 16. Suction pressure varying with uplift displacement rate

displacement rate. Those relationships were not linear, but can be quite well approximated by the power function $y = a(x)^{1/2}$. The best fits for experimental data were obtained with the following coefficients a: $a = 1.65$ for the ultimate capacity, $a = -1.32$ for the peak suction pressure, and $a = 1.21$ for the ultimate normalized displacement.

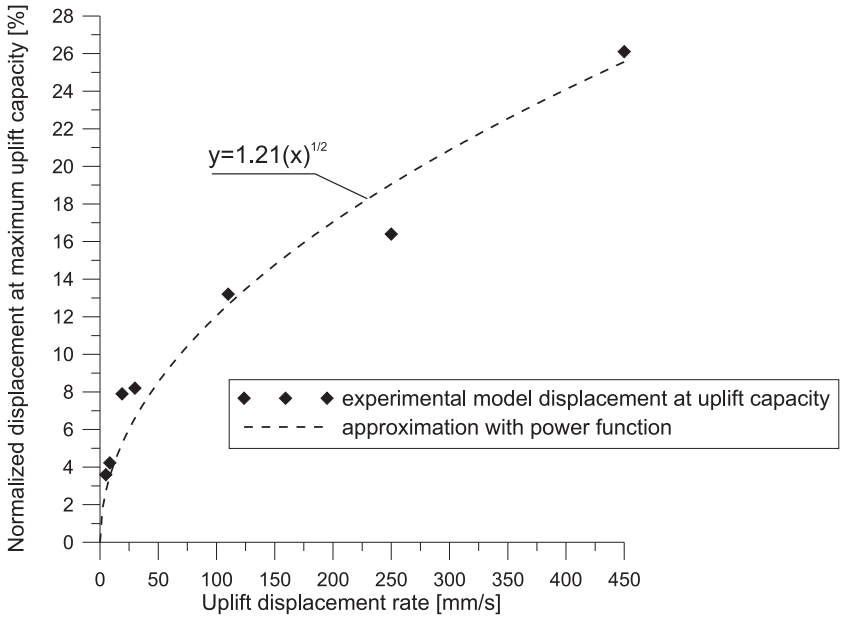

Fig. 17. Normalized uplift displacement at maximal uplift capacity varying with uplift displacement rate

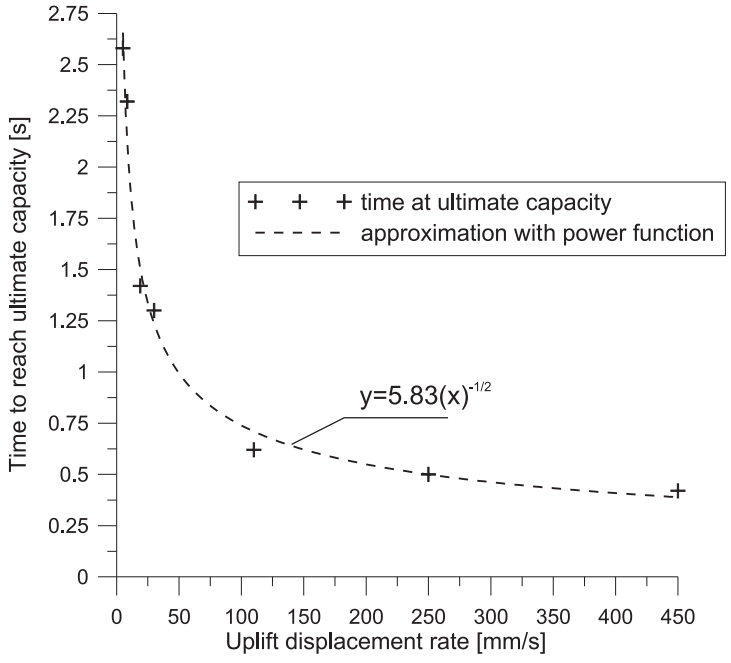

Fig. 18. Time at ultimate capacity varying with uplift displacement

The variation of time at ultimate capacity with the displacement rate is shown in Figure 18. In this case, the time values decreased markedly with increasing preset displacement rate. This relationship was not linear, either, and can be approximated by the power function $y = a(x)^{-1/2}$ with the coefficient $a = 5.83$.

5. Conclusions

1. The displacement rate significantly affects the magnitude of uplift resistance, as well as the magnitude of suction in the skirt compartment. The values of ultimate capacity and the absolute values of peak suction pressure increase significantly with increasing displacement rate. This relationship is not linear, but can be approximated by the power function $y = a(x)^{1/2}$.
2. The displacement rate has little effect on the stress-displacement relationship of the skirted foundation. The uplift capacity-displacement curve and the suction--displacement curve have similar shapes for all experimental displacement rates (like those observed in experimental studies carried out with lower displacement rates):
   – The uplift capacity increases rapidly before the peak value is reached, and then decreases gradually with continued pullout from the subsoil.
   – Changes in suction pressure developed during extraction are similar to those in uplift capacity.
   – The absolute values of suction are slightly smaller than the corresponding values of uplift capacity.
   – The maximum of uplift capacity and the maximum of suction beneath the lid occur at the same time.
3. The displacement rate significantly affects the duration of extraction, the duration of the initial stage of pullout, and the duration of the final stage of extraction. All these periods decrease significantly with increasing preset displacement rate.
4. The duration of the initial stage of pullout is considerably greater than the duration of the final stage at lower displacement rates. This difference decreases markedly for higher uplift rates.

References

Aderinto T., Li H. (2019) Review on Power Performance and Efficiency of Wave Energy Converters, *Energies*, **12** (22), 4329; https://doi.org/10.3390/en12224329.

Byrne B. W. (2000) *Investigation of Suction Caissons in Dense Sand*, PhD Dissertation, Magdalen College, University of Oxford, The United Kingdom.

Houlsby G. T., Kelly R. B., Byrne B. W. (2005b) The tensile capacity of suction caissons in sand under rapid loading, *Proc. Int. Symposium on Frontier in Offshore Geotechnics*, ISFOG, Perth, 405–410.

Hung L. C., Lee S., Tran N. X., Kim S.-R. (2017).Experimental investigation of the vertical pullout cyclic response of bucket foundations in sand., *Appl. Ocean Res.*, **68**, 325–335, //dx.doi.org/10.1016/j.apor.2017.06.006.

Kakasoltani S., Zeinoddini M., Abdi M. R., Arabzadeh H. (2011) An experimental investigation into the pull-out capacity of suction caissons in sand, *Proceedings of ASME 30th International Conference on Ocean, Offshore and Arctic Engineering*, 21–27.

Kelly R. B., Byrne B. W., Houlsby G. T., Martin C. M. (2004) Tensile Loading of Model Caisson Foundations for Structures on Sand, *Proceedings of the International Symposium of Offshore and Polar Engineering (ISOPE)*, 638–641.

Lehane B. M., Elkhatib S., Terzaghi S. (2014) Extraction of suction caissons in sand, *Géotechnique*, **64** (9), 735–739, DOI: 10.1680/geot.14.T.011.

Luke A. M., Rauc hA. F., Olson R. E., Mecham E. C. (2005) Components of Suction Caisson Capacity Measured in Axial Pullout Tests, *Journal of Ocean Engineering*, Elsevier, **22**, 878–891.

Mana D. S. K., Gourvenec S. M., Randolph M. F. (2014) Numerical modelling of seepage beneath skirted foundations subjected to vertical uplift, *Computers and Geotechnics*, **55**, 150–157, http://dx.doi.org/10.1016/j.compgeo.2013.08.007.

Manzotti E., Vaitkunaite E., Ibsen L. B. (2014) *Present knowledge about laboratory testing of axial loading on suction caissons*, Department of Civil Engineering, Aalborg University, DCE Technical Memorandum No. 42.

Ostrowski R., Schönhofer J., Szmytkiewicz P. (2016) South Baltic representative coastal field surveys, including monitoring at the Coastal Research Station in Lubiatowo, Poland, *Journal of Marine Systems*, **162**, 89–97.

Rahman M. S., Wang J., Deng W., Carter J. P. (2001) A neural network model for the uplift capacity of suction caissons, *Computers and Geotechnics*, **28** (4), 269–287, DOI: 10.1016/S0266-352X(00)00033-1.

Randolph M. F., Gaudin Ch., Gourvenec S. M., White D. J., Boylan N., Cassidy M. J. (2011) Recent advances in offshore geotechnics for deep water oil and gas developments, *Ocean Engineering*, **38** (7), 818–834, https://doi.org/10.1016/j.oceaneng.2010.10.021.

Sawicki A., Wachowski Ł., Kulczykowski M. (2016) The pull-out capacity of suction caissons in model investigations, *Archives of Hydro-Engineering and Environmental Mechanics*, **63** (2–3), 157–171, DOI: https://doi.org/10.1515/heem-2016-0010.

Senders M. (2008) *Suction Caissons in Sand as Tripod Foundations for Offshore Wind Turbines*, PhD Dissertation, School of Civil and Resource Engineering. University of Western Australia.

Shen K, Zhang, Y, Klinkvort R. T., Sturm H., Jostad H. P., Sivasithamparam N., Guo Z. (2017) Numerical Simulation of Suction Bucket Under Vertical Tension Loading, *Offshore Site Investigation Geotechnics*, 8th International Conference Proceeding, 488–497 (10), Society for Underwater Technology, https://doi.org/10.3723/OSIG17.488.

Thieken K., Achmus M, Schröder Ch. (2014) On the behavior of suction buckets in sand under tensile loads, *Computers and Geotechnics*, **60**, 88–100, http://dx.doi.org/10.1016/j.compgeo.2014.04.004.

Tjelta T. I. (2015) The suction foundation technology, Frontiers in Offshore Geotechnics III- Meyer (Ed.), *Proceedings of the Third International Symposium on Frontiers in Offshore Geotechnics (ISFOG 2015)*, Taylor & Francis Group, London, 85–93.

Wang X, Zeng X., Li J. (2019) Vertical performance of suction bucket foundation for offshore wind turbines in sand, *Ocean Engineering*, **180**, 40–48, https://doi.org/10.1016/j.oceaneng.2019.03.049.

Xie L., Mas S., Lin T. (2020) The seepage and Soil Plug Formation in Suction caissons in sand Using Visual Tests, *Applied Sciences*, **10**, 566.

Zhai H., Li D. (2017) Experimental Studies on Modified Suction Caissons in Fine Sand Subject to Uplift Loading, *Trans. Tianjin Univ.*, **23**, 562–569, DOI 10.1007/s12209-017-0085-7.

Zhou X. X., Chow Y. K., Leung C.F. (2008) Numerical modeling of breakout process of objects lying on seabed surface, *Computers and Geotechnics*, **35**, 686–702.